

# Improving Unsupervised Image Clustering With Robust Learning

Sungwon Park<sup>\*1,2</sup>, Sungwon Han<sup>\*1,2</sup>, Sundong Kim<sup>2</sup>, Danu Kim<sup>1,2</sup>,  
Sungkyu Park<sup>2</sup>, Seunghoon Hong<sup>1</sup>, Meeyoung Cha<sup>2,1</sup>

<sup>1</sup>School of Computing, KAIST, South Korea

<sup>2</sup>Data Science Group, IBS, South Korea

{psw0416, lion4151, danu, seunghoon.hong}@kaist.ac.kr {sundong, shaun01, mcha}@ibs.re.kr

## Abstract

Unsupervised image clustering methods often introduce alternative objectives to indirectly train the model and are subject to faulty predictions and overconfident results. To overcome these challenges, the current research proposes an innovative model *RUC* that is inspired by robust learning. *RUC*'s novelty is at utilizing pseudo-labels of existing image clustering models as a noisy dataset that may include misclassified samples. Its retraining process can revise misaligned knowledge and alleviate the overconfidence problem in predictions. This model's flexible structure makes it possible to be used as an add-on module to state-of-the-art clustering methods and helps them achieve better performance on multiple datasets. Extensive experiments show that the proposed model can adjust the model confidence with better calibration and gain additional robustness against adversarial noise.

## 1. Introduction

Unsupervised clustering is a core task in computer vision that aims to identify each image's class membership without using any labels. Here, a class represents the group membership of images that share similar visual characteristics. Many studies have proposed deep learning-based algorithms that utilize distance in feature space as a similarity metric to assign data points into classes [10, 43].

Training without ground-truth guidance, however, is prone to finding trivial solutions that are learned from low-level visual traits like colors and textures [21]. Several studies have introduced innovative ways to guide the model's training indirectly by setting alternative objectives. For example, Hu et al. [19] proposed to maximize the mutual information between input and its hidden representations, and Ji et al. [21] proposed to learn invariant features against data augmentation. Entropy-based balancing has often been

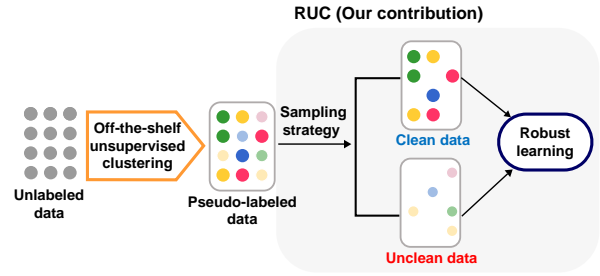


Figure 1: Illustration for this work's basic concept: robust learning approach via clean sample selection using pseudo-labels from unsupervised clustering algorithm.

adopted to prevent degenerate solutions along with these kinds of objectives [16, 21, 41].

Nevertheless, these alternative objectives are bound to producing overconfident results, i.e., low-entropy predictions, due to the dense grouping among clusters. When uncertain samples are added to a wrong cluster at an early stage of training, the model gradually becomes overconfident in its later predictions as the noise from misclassification accumulates and degrades the overall performance.

This paper introduces a novel robust learning training method, *RUC* (Robust learning for Unsupervised Clustering), that runs in conjunction with existing clustering models to alleviate the noise discussed above. Utilizing and treating the existing clustering model's results as a noisy dataset that may include wrong labels, *RUC* updates the model's misaligned knowledge. Bringing insights from the literature, we filter out unclean samples and apply loss correction (see Fig. 1). This process is assisted by label smoothing and co-training to reduce any wrong gradient signal from unclean labels. This retraining process with revised pseudo-labels further regularizes the model and prevents producing overconfident results.

*RUC* comprises of two key components: (1) extracting clean samples and (2) retraining with the refined dataset. We propose confidence-based, metric-based, and hybrid

<sup>\*</sup>Equal contribution to this work.

strategies in filtering out misclassified pseudo-labels. The first approach considers samples of high prediction confidence from the original clustering model as a clean set; it filters out low confidence samples. This strategy relies on the model’s calibration performance. The second approach utilizes similarity metrics from unsupervised embedding models to detect clean samples with non-parametric classifiers by checking whether the given instance shares the same labels with top  $k$ -nearest samples. The third approach combines the two and selects samples that are credible according to both strategies.

The next step is to retrain the clustering model with the sampled dataset. We use MixMatch [4], a semi-supervised learning technique; which uses clean samples as labeled data and unclean samples as unlabeled data. We also adopt label smoothing to leverage strong denoising effects on the label noise [28] and block learning from overconfident samples [21, 41]. Finally, a co-training architecture with two networks is used to mitigate noise accumulation from the unclean samples during training and increase performance.

We evaluate RUC with rigorous experiments on datasets, including CIFAR-10, CIFAR-20, and STL-10. Combining RUC to an existing clustering model outperforms the state-of-the-art results with the accuracy of 90.3% in CIFAR-10, 54.3% in CIFAR-20, and 86.7% in STL-10 dataset. RUC also enhances the baseline model to be robust against adversarial noise. We summarize contributions as follows:

- The proposed algorithm RUC aids existing unsupervised clustering models via retraining and avoiding overconfident predictions.
- The unique retraining process of RUC helps existing models boost performance. It achieves a 5.3pp increase for the STL-10 dataset when added to the state-of-the-art model (81.4% to 86.7%).
- The ablation study shows every component in RUC is critical, including the three proposed strategies (i.e., confidence-based, metric-based, and hybrid) that excel in extracting clean samples from noisy pseudo-labels.
- The proposed training process is robust against adversarial noise and can adjust the model confidence with better calibrations.

Implementation details of the model and codes are available via <https://github.com/deu30303/RUC>.

## 2. Related Work

### 2.1. Unsupervised Image Clustering

The main objective of clustering is to group the data points into distinct classes of similar traits [20]. Most real-world problems deal with high dimensional data (e.g., images), and thereby, setting a concrete notion of similarity while extracting low-dimensional features becomes key components for setting appropriate standards for group-

ing [48]. Likewise, unsupervised clustering is a line of research aiming to tackle both dimensionality reduction and boundary identification over the learned similarity metric [16]. Existing research can be categorized into *sequential*, *joint*, and *multi-step refinement approach*.

**Sequential approach.** Sequential approach extracts features, then sequentially applies the conventional distance or density-based clustering algorithm for class assignments. For example, Ding et al. [10] use principal component analysis to extract low-dimensional features and then apply  $k$ -means clustering to assign classes. For feature extraction, autoencoder structures are often used to extract latent features before grouping, types of autoencoder include stacked [43], boolean [2], or variational autoencoder [23]. However, these models tend to produce features with little separation among clusters due to the lack of knowledge on subsequent assignment processes.

**Joint approach.** The joint approach’s characteristic is to use an end-to-end pipeline that concurrently performs feature extraction and class assignment. An example is Yang et al. [50], which adopt the concept of clustering loss to guarantee enough separations among clusters. End-to-end CNN pipelines are used widely to iteratively identify clusters while refining extracted features [5, 7, 48]. Recent studies have shown that a mutual information-based objective is an effective measure to improve classification accuracy [19, 21]. Nonetheless, those models still bear a problem of generating unintended solutions that depend on trivial low-level features from random initialization [16].

**Multi-step refinement approach.** To mitigate the unintended trivial solutions, recent approaches leverage the power of unsupervised embedding learning models to provide better initialization for downstream clustering tasks [8, 47, 49]. These methods generate feature representations to gather data points with similar visual traits and push away the rest in an embedding space. With the initialization, clustering results are elaborated in a refinement step, bringing significant gain in its class assignment quality [16, 41]. In particular, SCAN [41] first obtains high-level feature representations by feature similarity then clusters those representations by nearest neighbors, and this model has shown remarkable performance on unsupervised clustering.

**Add-on modules to improve unsupervised clustering.** The proposed retraining process with sample selection strategy improves off-the-shelf unsupervised clustering algorithms (e.g., sequential, joint, multi-step refinement) by acting as an add-on module. Our module’s main objective is to revise the misaligned knowledge of trained clustering models via label cleansing and retraining with the refined labels. This method has not been well investigated before but has begun to be proposed recently. Gupta et al. [13] show that semi-supervised retraining improves unsupervised clustering. They draw a graph where data samples are nodes, and

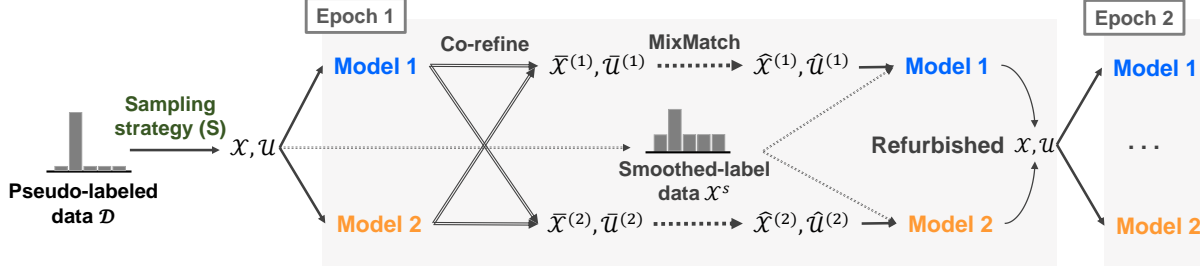


Figure 2: Illustration of the proposed model. Our model first selects clean samples as a labeled dataset  $\mathcal{X}$  and considers the remaining samples as an unlabeled dataset  $\mathcal{U}$  (Section 3.1). Next, we train two networks  $f_{\theta(1)}$  and  $f_{\theta(2)}$  in a semi-supervised fashion (Section 3.2). In each epoch, the MixMatch algorithm, along with co-training and label smoothing, is applied for training. The clean set is updated via co-refurbishing for the next epoch.

the confidence from ensemble models between the samples is an edge. Then, a dense sub-graph is considered as a clean set. In contrast, we introduce a robust learning approach to divide pseudo-labels into a clean and unclean set and train the model while avoiding faulty gradient signals from unclean samples.

## 2.2. Robust Learning With Label Noise

A widely used setting for robust learning is where an adversary has deliberately corrupted the labels, which otherwise arise from some clean distribution [32, 39]. According to the literature, deep networks easily overfit to the label noise during training and get a low generalization power [27]. In this light, models that prevent overfitting in a noise label environment have been studied.

**Loss correction.** The first representative line of work is a loss correction, which relabels unclean samples explicitly or implicitly. For example, Patrini et al. [34] estimate the label transition probability matrix to correct the loss and retrain the model. To estimate the transition matrix more accurately, the gold loss correction approach [18] is proposed to utilize trusted labels as additional information.

**Loss reweighting.** The next line of work is loss reweighting, which aims to give a smaller weight to the loss of unclean samples so that model can reduce the negative effect of label noise during training. One work computes the importance as an approximated ratio of two data distributions; clean and unclean [45]. On the other hand, the active bias approach [6] calculates the inconsistency of predictions during training and assigns a weight to penalize unclean data.

**Sample selection.** Relabeling the misclassified samples can instead cause a false correction. In this context, many recent works introduce a sample selection approach that filters out misclassified samples and only selects clean data for training [29, 31]. Notably, the small loss trick, which regards the sample with small training loss as clean, shows a powerful ability to separate true- and false-labeled data

points [1, 22, 27]. Also, recent studies suggest diverse ways to lead additional performance by maintaining two networks to avoid accumulating sampling bias [15, 52], adopting refurbishment of false-labeled samples [38], or using a semi-supervised approach to utilize false-labeled sample maximally [26]. Our model advances some of these sample selection approaches to filter out unclean samples out of clustering results and utilize clean samples only during retraining.

## 3. Method

RUC is an add-on method that can be used in conjunction with the existing unsupervised clustering methods to refine mispredictions. Its key idea is at utilizing the initial clustering results as *noisy* pseudo-labels and learning to refine them with a mild clustering assumption [40] and techniques from the robust learning [26, 28].

Figure 2 and Algorithm 1 illustrate the overall pipeline of the proposed algorithm. Given the initial pseudo-labels, we first divide the training data into the two disjoint sets: clean and unclean (Section 3.1). Then treating these sets each as labeled and unlabeled data, we learn a classifier in a semi-supervised manner while refurbishing the labeled and unlabeled data (Section 3.2). We guide the semi-supervised class assignment with robust learning techniques, such as co-training and label smoothing, to account for inherent label noises. These techniques are useful in handling label noises and calibrating the model’s prediction score. Below we describe the model details.

### 3.1. Extracting Clean Samples

Let  $\mathcal{D} = \{(\mathbf{x}_i, \mathbf{y}_i)\}_{i=1}^N$  denotes the training data, where  $\mathbf{x}_i$  is an image and  $\mathbf{y}_i = g_\phi(\mathbf{x}_i)$  is a pseudo-label from an unsupervised classifier  $g_\phi$ . The model first divides the pseudo-labels into two disjoint sets as  $\mathcal{D} = \mathcal{X} \cup \mathcal{U}$  with a specified sampling strategy. We consider  $\mathcal{X}$  as clean, whose pseudo-labels are moderately credible and thus can

---

**Algorithm 1** Robust learning algorithm using unsupervised clustering pseudo-label.

---

**Input:** Sampling strategy  $\mathcal{S}$ , training dataset with pseudo-labels  $\mathcal{D}$ , two networks  $f_{\theta^{(1)}}$ ,  $f_{\theta^{(2)}}$ , sharpening temperature  $T$ , number of augmentations  $M$ , unsupervised loss weight  $\lambda_{\mathcal{U}}$ , refurbish threshold  $\tau_2$ , weak- and strong augmentation  $\phi_a$ ,  $\phi_A$

```
/* Divide the dataset  $\mathcal{D}$  into clean and noisy set using a sampling strategy */
 $\mathcal{X}, \mathcal{U} = \mathcal{S}(\mathcal{D})$  (i.e.  $\mathcal{X} = \{(\mathbf{x}_b, \mathbf{y}_b) : b \in (1, \dots, B)\}, \mathcal{U} = \{\mathbf{u}_b : b \in (1, \dots, B)\}$ )
for  $k \in \{1, 2\}$  do
    /* Train the two networks  $f_{\theta^{(1)}}$  and  $f_{\theta^{(2)}}$  iteratively */
    for  $b \in \{1, \dots, B\}$  do
         $\tilde{\mathbf{y}}_b = (1 - \epsilon) \cdot \mathbf{y}_b + \frac{\epsilon}{(C-1)} \cdot (\mathbf{1} - \mathbf{y}_b)$  // Inject uniform noise into all classes (label smoothing)
        for  $m \in \{1, \dots, M\}$  do
             $\mathbf{x}_{b,m}, \mathbf{u}_{b,m} = \phi_a(\mathbf{x}_b), \phi_a(\mathbf{u}_b)$  // Perform weak augmentation  $M$  times
        end
         $\bar{\mathbf{y}}_b = (1 - w_b^{(c)}) \cdot \mathbf{y}_b + w_b^{(c)} \cdot f_{\theta^{(c)}}(\mathbf{x}_b)$  // Refine the labels ( $(c)$  denotes the counter network)
         $\bar{\mathbf{y}}_b = \text{Sharpen}(\bar{\mathbf{y}}_b, T)$  // Apply sharpening to the refined label
         $\bar{\mathbf{q}}_b = \frac{1}{2M} \sum_m (f_{\theta^{(1)}}(\mathbf{u}_{b,m}) + f_{\theta^{(2)}}(\mathbf{u}_{b,m}))$  // Ensemble both networks' predictions to guess labels
         $\bar{\mathbf{q}}_b = \text{Sharpen}(\bar{\mathbf{q}}_b, T)$  // Apply sharpening to the guessed labels
    end
     $\mathcal{X}^s = \{(\phi_A(\mathbf{x}_b), \tilde{\mathbf{y}}_b) : b \in \{1, \dots, B\}\}$  // Strongly augmented samples with smoothed labels
     $\bar{\mathcal{X}}^{(k)} = \{(\mathbf{x}_b, \bar{\mathbf{y}}_b) : b \in \{1, \dots, B\}\}$  // Co-refined labeled samples
     $\bar{\mathcal{U}}^{(k)} = \{(\mathbf{u}_b, \bar{\mathbf{q}}_b) : b \in \{1, \dots, B\}\}$  // Co-refined unlabeled samples
     $\hat{\mathcal{X}}^{(k)}, \hat{\mathcal{U}}^{(k)} = \text{MixMatch}(\bar{\mathcal{X}}^{(k)}, \bar{\mathcal{U}}^{(k)})$  // Apply MixMatch
     $\mathcal{L}_t = \mathcal{L}_{\mathcal{X}^s} + \mathcal{L}_{\hat{\mathcal{X}}} + \lambda_{\mathcal{U}} \mathcal{L}_{\hat{\mathcal{U}}}$  // Calculate the total loss
     $\mathcal{X} \leftarrow \mathcal{X} \cup \text{Co-Refurbish}(\bar{\mathcal{U}}, f_{\theta^{(k)}}, \tau_2)$  // Refurbish noisy samples to clean samples (Eq. (18), (19))
     $\theta^{(k)} \leftarrow \text{SGD}(\mathcal{L}_t, \theta^{(k)})$  // Update network parameters
end
```

---

be used as a labeled dataset  $(\mathbf{x}, \mathbf{y}) \in \mathcal{X}$  for refinement. In contrast, we consider  $\mathcal{U}$  as unclean, whose labels we discard  $\mathbf{u} \in \mathcal{U}$ . Designing an accurate sampling strategy is not straightforward, as there is no ground-truth to validate the pseudo-labels directly. Motivated by robust learning's clean set selection strategy, we explore three different approaches: (1) confidence-based, (2) metric-based, and (3) hybrid.

**Confidence-based strategy.** This approach selects clean samples based on the confidence score of an unsupervised classifier. Given a training sample  $(\mathbf{x}, \mathbf{y}) \in \mathcal{D}$ , we consider the pseudo-label  $\mathbf{y}$  is credible if  $\max(\mathbf{y}) > \tau_1$ , and add it to the clean set  $\mathcal{X}$ . Otherwise, it is assigned to  $\mathcal{U}$ . This is motivated by the observation that the unsupervised classifier tends to generate overconfident predictions; thus, we trust only the most typical examples from each class while ignoring the rest. The threshold  $\tau_1$  is set substantially high to eliminate as many uncertain samples as possible.

**Metric-based strategy.** The limitation of the above approach is that the selection strategy still entirely depends on the unsupervised classifier. This approach leverages an additional embedding network  $h_\psi$  learned in an unsupervised manner (e.g., SimCLR [8]) and measures the credibility of the pseudo-label based on how well it coincides to the classification results using  $h_\psi$ . For each  $(\mathbf{x}, \mathbf{y}) \in \mathcal{D}$ , we compute its embedding  $h_\psi(\mathbf{x})$ , and apply the non-

parameteric classifier based on k-Nearest Neighbor (kNN) by  $\mathbf{y}' = \text{kNN}(h_\psi(\mathbf{x}))$ . We consider that the pseudo-label is credible if  $\arg\max(\mathbf{y}) = \arg\max(\mathbf{y}')$  and add it to the clean set  $\mathcal{X}$ . Otherwise, it is assigned to the unclean set  $\mathcal{U}$ .

**Hybrid strategy.** This approach will add a sample to the clean set  $\mathcal{X}$  only if it is considered credible by both confidence-based and metric-based strategies. All other samples are added to  $\mathcal{U}$ .

### 3.2. Retraining via Robust Learning

Given a clean set  $\mathcal{X}$  and an unclean set  $\mathcal{U}$ , our next step aims to learn the refined classifier  $f_\theta$  that revises incorrect predictions of the initial unsupervised classifier.

**Vanilla semi-supervised learning.** A naive baseline is to consider  $\mathcal{X}$  as labeled data and  $\mathcal{U}$  as unlabeled data each to train a classifier  $f_\theta$  using semi-supervised learning techniques. We utilize MixMatch [4] as a baseline<sup>1</sup>.

MixMatch is a semi-supervised algorithm that estimates low-entropy mixed labels from unlabeled examples using MixUp augmentation [54]. For unsupervised clustering, MixUp can bring additional resistance against noisy labels since a large amount of extra virtual examples from MixUp

---

<sup>1</sup>Note that our method is not dependent on the particular choice of the semi-supervised learning method and can incorporate the others.



interpolation makes memorization hard to achieve [26, 54]. Specifically, given a two paired data  $(\mathbf{x}_1, \mathbf{y}_1)$  and  $(\mathbf{x}_2, \mathbf{y}_2)$  sampled from either labeled or unlabeled data, it augments the data using the following operations.

$$\lambda \sim \text{Beta}(\alpha, \alpha) \quad (1)$$

$$\lambda' = \max(\lambda, 1 - \lambda) \quad (2)$$

$$\mathbf{x}' = \lambda' \mathbf{x}_1 + (1 - \lambda') \mathbf{x}_2 \quad (3)$$

$$\mathbf{y}' = \lambda' \mathbf{y}_1 + (1 - \lambda') \mathbf{y}_2. \quad (4)$$

In case of unlabeled data  $\mathbf{u} \in \mathcal{U}$ , MixMatch is employed such that a surrogate label  $\mathbf{y} = \mathbf{q}$  is obtained by averaging the model’s predictions over multiple augmentations after sharpening [4]. Later, we will show that using the labels  $\mathbf{y}$  and  $\mathbf{q}$  directly in semi-supervised learning leads to a sub-optimal solution and discuss how to improve its robustness.

For  $\hat{\mathcal{X}}$  and  $\hat{\mathcal{U}}$  after MixMatch (Eq. (5)), a vanilla semi-supervised learning model trains with two separate losses: the cross-entropy loss for the labeled set  $\hat{\mathcal{X}}$  (Eq. (6)), and the consistency regularization for the unlabeled set  $\hat{\mathcal{U}}$  (Eq. (7)).  $H(p, q)$  denotes the cross-entropy between  $p$  and  $q$ .

$$\hat{\mathcal{X}}, \hat{\mathcal{U}} = \text{MixMatch}(\mathcal{X}, \mathcal{U}) \quad (5)$$

$$\mathcal{L}_{\hat{\mathcal{X}}} = \frac{1}{|\hat{\mathcal{X}}|} \sum_{\hat{\mathbf{x}}, \hat{\mathbf{y}} \in \hat{\mathcal{X}}} H(\hat{\mathbf{y}}, f_{\theta}(\hat{\mathbf{x}})) \quad (6)$$

$$\mathcal{L}_{\hat{\mathcal{U}}} = \frac{1}{|\hat{\mathcal{U}}|} \sum_{\hat{\mathbf{u}}, \hat{\mathbf{q}} \in \hat{\mathcal{U}}} \|\hat{\mathbf{q}} - f_{\theta}(\hat{\mathbf{u}})\|_2^2 \quad (7)$$

**Label smoothing.** To regularize our model being overconfident to the noisy prediction, we apply the label smoothing along with vanilla semi-supervised learning. Label smoothing prescribes soft labels by mixing in a uniform noise, and improves the calibration of the prediction [28]. Given a labeled sample with its corresponding label  $(\mathbf{x}, \mathbf{y}) \in \mathcal{X}$ , we inject uniform noise into all classes as follows:

$$\tilde{\mathbf{y}} = (1 - \epsilon) \cdot \mathbf{y} + \frac{\epsilon}{(C - 1)} \cdot (\mathbf{1} - \mathbf{y}) \quad (8)$$

where  $C$  is the number of class and  $\epsilon \sim \text{Uniform}(0, 1)$  is the noise. We compute the cross-entropy using the soft label  $\tilde{\mathbf{y}}$  and the predicted label of the strongly augmented sample  $\phi_A(\mathbf{x})$  via RandAugment [9]. We found that strong augmentations minimize the memorization from noise samples.

$$\mathcal{L}_{\mathcal{X}^s} = \frac{1}{|\mathcal{X}|} \sum_{\mathbf{x}, \tilde{\mathbf{y}} \in \mathcal{X}} H(\tilde{\mathbf{y}}, f_{\theta}(\phi_A(\mathbf{x}))) \quad (9)$$

Our final objective for training can be written as:

$$\mathcal{L}(\theta; \mathcal{X}, \hat{\mathcal{X}}, \hat{\mathcal{U}}) = \mathcal{L}_{\mathcal{X}^s} + \mathcal{L}_{\hat{\mathcal{X}}} + \lambda_{\mathcal{U}} \mathcal{L}_{\hat{\mathcal{U}}}, \quad (10)$$

where  $\lambda_{\mathcal{U}}$  is a hyper-parameter to control the effect of the unsupervised loss in MixMatch.

**Co-training.** Maintaining a single network for learning has a vulnerability of overfitting to incorrect pseudo-labels, since the initial error from the network is transferred back again, and thereby, accumulated [15]. To avoid this fallacy, we additionally introduce a co-training module where the two networks  $f_{\theta(1)}, f_{\theta(2)}$  are trained in parallel and exchange their guesses for teaching each other by adding co-refinement on top of MixMatch.

Co-refinement is a label refinement process that aims to produce reliable labels by incorporating both networks’ predictions. Following the previous literature [26], we apply co-refinement both on the label set  $\mathcal{X}$  and the unlabeled set  $\mathcal{U}$  for each network. Here, we explain the co-refinement process from the perspective of  $f_{\theta(1)}$ . For the labeled data point  $\mathbf{x}$ , we calculate the linear sum between the original label  $\mathbf{y}$  in  $\mathcal{X}$  and the prediction from the counter network  $f_{\theta(2)}$  (Eq. (11)) and apply sharpening on the result to generate the refined label  $\bar{\mathbf{y}}$  (Eq. (12)).

$$\bar{\mathbf{y}} = (1 - w^{(2)}) \cdot \mathbf{y} + w^{(2)} \cdot f_{\theta(2)}(\mathbf{x}) \quad (11)$$

$$\bar{\mathbf{y}} = \text{Sharpen}(\bar{\mathbf{y}}, T), \quad (12)$$

where  $w^{(2)}$  is the counter network’s confidence value of  $\mathbf{x}$ , and  $T$  is the sharpening temperature. For the unlabeled set  $\mathcal{U}$ , we apply an ensemble of both networks’ predictions to guess the pseudo-label  $\bar{\mathbf{q}}$  of data sample  $\mathbf{u}$  as follows:

$$\bar{\mathbf{q}} = \frac{1}{2M} \sum_m (f_{\theta(1)}(\mathbf{u}_m) + f_{\theta(2)}(\mathbf{u}_m)) \quad (13)$$

$$\bar{\mathbf{q}} = \text{Sharpen}(\bar{\mathbf{q}}, T), \quad (14)$$

where  $\mathbf{u}_m$  is  $m$ -th weak augmentation of  $\mathbf{u}$ .

In place of  $\mathcal{X}$  and  $\mathcal{U}$ , co-refinement produces the refined dataset  $(\mathbf{x}, \bar{\mathbf{y}}) \in \bar{\mathcal{X}}^{(1)}$ , and  $(\mathbf{u}, \bar{\mathbf{q}}) \in \bar{\mathcal{U}}^{(1)}$  through Eq. (11) to (14). We utilize those datasets as an input for MixMatch algorithm, and the model is eventually optimized as follows:

$$\bar{\mathcal{X}}^{(1)}, \bar{\mathcal{U}}^{(1)} = \text{Co-refinement}(\mathcal{X}, \mathcal{U}, \theta^{(1)}, \theta^{(2)}) \quad (15)$$

$$\hat{\mathcal{X}}^{(1)}, \hat{\mathcal{U}}^{(1)} = \text{MixMatch}(\bar{\mathcal{X}}^{(1)}, \bar{\mathcal{U}}^{(1)}) \quad (16)$$

$$\theta^{(1)} \leftarrow \arg \min_{\theta^{(1)}} \mathcal{L}(\theta^{(1)}; \mathcal{X}, \hat{\mathcal{X}}^{(1)}, \hat{\mathcal{U}}^{(1)}), \quad (17)$$

where  $\mathcal{L}$  is the loss defined in Eq. (10). This process is also conducted for  $f_{\theta(2)}$  in a same manner.

**Co-refurbishing.** Lastly, we refurbish the noise samples at the end of every epoch to deliver the extra clean samples across the training process. If at least one of the networks’ confidence on the given unclear sample  $\mathbf{u} \in \mathcal{U}$  is over the threshold  $\tau_2$ , the corresponding sample’s label is updated with the network’s prediction  $\mathbf{p}$ . The updated sample is then regarded as clean and appended to the labeled set  $\mathcal{X}$ .

$$\mathbf{p} = f_{\theta(k)}(\mathbf{u}), \text{ where } k = \arg \max_{k'} (\max(f_{\theta(k')}(\mathbf{u}))) \quad (18)$$

$$\mathcal{X} \leftarrow \mathcal{X} \cup \{(\mathbf{u}, \mathbf{1}_{\mathbf{p}}) | \max(\mathbf{p}) > \tau_2\}, \quad (19)$$

where  $\mathbb{1}_{\mathbf{p}}$  is a one-hot vector of  $\mathbf{p}$  whose  $i$ -th element is 1, considering  $i = \arg \max(\mathbf{p})$ .

## 4. Experiments

For evaluation, we first compared the performance of our model against other baselines over multiple datasets. Then, we examined each component’s contribution to performance improvement. Lastly, we investigated how RUC helps improve existing clustering models in terms of their confidence calibration and robustness against adversarial attacks.

### 4.1. Unsupervised Image Clustering Task

**Settings.** Three benchmark datasets were used. The first two are CIFAR-10 and CIFAR-100, which contain 60,000 images of 32x32 pixels. For CIFAR-100, we utilized 20 superclasses following previous works [41]. The last is STL-10, containing 100,000 unlabeled images and 13,000 labeled images of 96x96 pixels. For the clustering problem, only the 13,000 labeled images were used.

Our model employed the ResNet18 [17] architecture following other baselines [16, 21, 41] and the model was trained for 200 epochs. Initial confidence threshold  $\tau_1$  was set as 0.99, and the number of neighbors  $k$  to divide the clean and noise samples was set to 100. The threshold  $\tau_2$  for refurbishing started from 0.9 and increased by 0.02 in every 40 epochs. The label smoothing parameter  $\epsilon$  was set to 0.5. For evaluating the class assignment, the Hungarian method [24] was used to map the best bijection permutation between the predictions and ground-truth.

**Result.** Table 1 shows the overall performances of clustering algorithms over three datasets: CIFAR-10, CIFAR-20, and STL-10. For these datasets, the proposed model RUC, when applied to the SCAN [41] algorithm, outperforms all other baselines. Particularly, for STL-10, the combined model shows a substantial improvement of 5.3pp. Furthermore, RUC achieves consistent performance gain over another clustering model, TSUC [16]. These results indicate that our model can be applied to various other existing clustering algorithms. We also confirm that all three selection strategies (i.e., confidence-based, metric-based, and hybrid) bring considerable performance improvement.

### 4.2. Component Analyses

To evaluate the model’s efficacy, we conduct an ablation study by repeatedly assessing its performance after removing each component. We also evaluate the accuracy of different selection and refurbishing strategies based on precision, recall, and F1 score.

**Ablation study.** The proposed model utilizes two robust learning techniques to cope with unclear samples effectively: co-training and label smoothing. We remove each

Method	CIFAR-10	CIFAR-20	STL-10
$k$ -means [44]	22.9	13.0	19.2
Spectral clustering [53]	24.7	13.6	15.9
Triplets [36]	20.5	9.9	24.4
Autoencoder (AE) [3]	31.4	16.5	30.3
Variational Bayes AE [23]	29.1	15.2	28.2
GAN [35]	31.5	15.1	29.8
JULE [51]	27.2	13.7	27.7
DEC [48]	30.1	18.5	35.9
DAC [7]	52.2	23.8	47.0
DeepCluster [5]	37.4	18.9	33.4
ADC [14]	32.5	16.0	53.0
IIC [21]	61.7	25.7	49.9
TSUC† [16]	80.2	35.5	62.0
SCAN† [41]	88.7	50.6	81.4
TSUC + RUC (Confidence)	81.8 / 82.5	39.6 / 40.6	65.1 / 65.5
TSUC + RUC (Metric)	82.5 / 82.9	39.5 / 40.4	66.3 / 66.6
TSUC + RUC (Hybrid)	82.1 / 82.8	39.5 / 40.6	66.0 / 66.8
SCAN + RUC (Confidence)	<b>90.3</b> / 90.3	53.3 / 53.5	<b>86.7</b> / 86.8
SCAN + RUC (Metric)	89.5 / 89.5	53.9 / 53.9	84.7 / 85.1
SCAN + RUC (Hybrid)	90.1 / 90.1	<b>54.3</b> / 54.5	86.6 / 86.7

Table 1: Performance improvement with RUC (accuracy presented in percent). Baseline results are excerpted from [16, 41] and we report the last/best accuracy. †Results obtained from our experiments with official code.

component from the full model to assess their efficacy. Table 2 shows the classification accuracy of each ablation on the STL-10 dataset. RUC with all components performs the best, implying that dropping any component results in performance degradation. We also compare a variant, which drops both label smoothing and co-training (i.e., MixMatch only). The effect of co-training is not evident in Table 2. Nevertheless, it improved the performance from 36.3 to 39.6 for the lowest noise ratio CIFAR-20 pseudo-labels when we set the base model as TSUC. This finding may suggest that co-training is more effective for pseudo-labels with high noise ratios. The co-training structure showed additional stability in training.<sup>2</sup>

Setup	Last Acc	Best Acc
RUC with all components	<b>86.7</b>	<b>86.8</b>
without co-training	86.2	86.4
without label smoothing	85.5	85.8
with MixMatch only	85.2	85.4

Table 2: Ablation results of the SCAN+RUC on STL-10.

**Comparison between add-on robust learning modules: RUC and DivideMix.** As an alternative of RUC, one may combine the extant robust learning model on top of

<sup>2</sup>Due to space limitation, we report findings on this on the supplementary material.

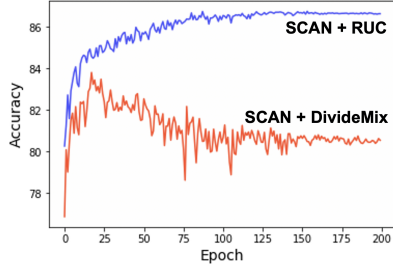


Figure 3: Changes of clustering accuracy across each epoch on STL-10.

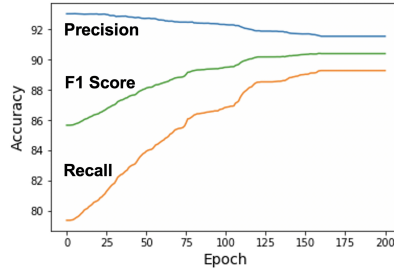


Figure 4: Changes of sampling accuracy across each epoch on our model.

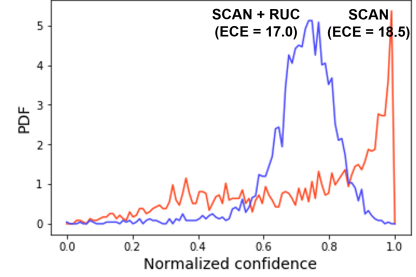


Figure 5: Confidence distribution for noise sample on STL-10.

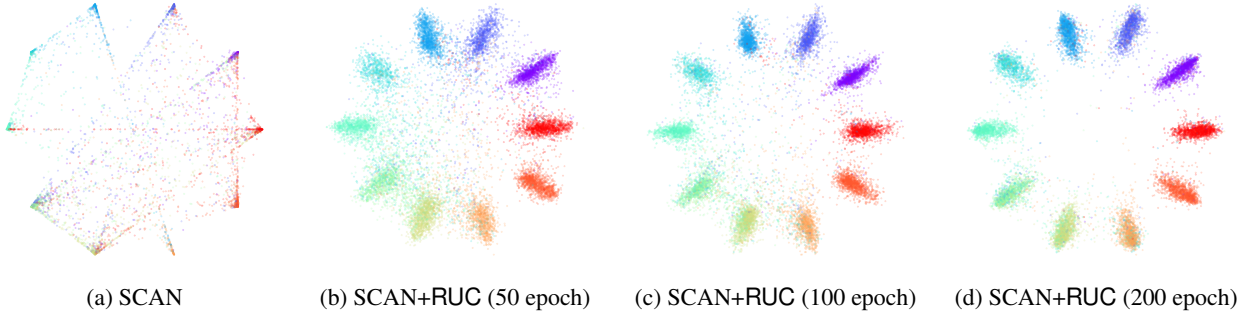


Figure 6: Visualization of clustering results on STL-10. The leftmost figure shows the results from the SCAN, while the right three figures display the intermediate results of our model on top of SCAN at different training epochs.

SCAN. We compare the performance between RUC and the state-of-the-art method in the robust learning domain, DivideMix [26]. The comparison of DivideMix and RUC in Figure 3 shows that DivideMix faces a drastic decline in accuracy after some epochs, whereas RUC maintains consistently high accuracy. This result may be due to the lack of separation in cross-entropy loss between the clean set and the unclean set for DivideMix, i.e., too many or little data points may have been selected by the algorithm.

**Sampling strategy analysis.** We next evaluate the quality of the clean set generated from three sampling strategies (See Table 3). Overall, the precision is higher for the hybrid strategy, whereas the recall is higher for the metric-based strategy. We also test the co-refurbish accuracy over the epochs. Figure 4 displays the change of precision, recall, and F1-score using confidence-based sampling on the STL-10 dataset for our model. The model’s precision drops slightly as the number of epoch increases, but the recall increases significantly. The F1-score, which shows the overall clean set sampling accuracy, increased about 5% over 200 epoch. It can be interpreted as a much higher rate of true-positive cases than the false-positive cases in the refurbished samples, which means that the model successfully corrects the misclassified unclean samples through the refurbishing. In a nutshell, the current hybrid selection strategy can distinguish clean sets relatively well since the selected samples

benefit from merits of both strategies. This strategy, however, cannot achieve the best performance. Further development of selection strategy will help to increase the performance of the proposed RUC model.

Strategy	CIFAR-10			CIFAR-20			STL-10		
	C	M	H	C	M	H	C	M	H
Precision	92.6	91.6	93.7	59.5	59.0	63.6	93.0	87.6	94.2
Recall	93.5	93.2	89.3	83.1	88.5	77.4	79.4	94.4	78.3
F1 Score	93.0	92.4	91.4	69.3	70.8	69.8	85.7	90.9	85.5

Table 3: Quality of the clean set (C : Confidence, M : Metric, H : Hybrid)

### 4.3. In-Depth Performance Analysis

So far, we showed that RUC improves existing baselines substantially, and its model components all contribute to the performance gain. We now examine RUC’s calibration effect and present a qualitative analysis by applying it to the state-of-the-art base model, SCAN. This subsection will also demonstrate the role of RUC in handling adversarially crafted noise.

**Confidence calibration.** Many unsupervised clustering algorithms are subject to overconfident results because of their entropy-based balancing [16, 41]. If a model is overconfident to noisy samples, separating the clean set and the

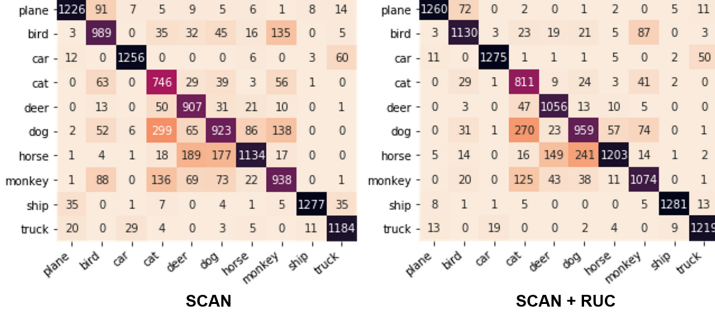


Figure 7: Confusion matrices of the SCAN and SCAN+RUC results on STL-10. The row names are predicted class labels, and the columns are the ground-truths.

unclean set becomes challenging, and this can induce the overall performance degradation. Figure 5 shows the calibration effect of RUC. SCAN’s confidence is highly concentrated near 1, while our model’s confidence is widely distributed over [0.6, 0.8]. We also report the degree of calibration quality using Expected Calibration Error (ECE) [12]:

$$\text{ECE} = \sum_{m=1}^M \frac{|B_m|}{n} |acc(B_m) - conf(B_m)|, \quad (20)$$

where  $n$  is the number of data points,  $B_m$  is the  $m$ -th group from equally spaced buckets based on the model confidence over the data points;  $acc(B_m)$  and  $conf(B_m)$  are average accuracy and confidence over  $B_m$  respectively. Lower ECE of RUC in Figure 5 implies that our add-on process leads to better calibrations.

To observe this effect more clearly, we visualize the clustering confidence result at different training epochs in Figure 6. Unlike the result of SCAN in which the overly clustered sample and the uncertain sample are mixed, the result of SCAN+RUC shows that the sample’s class distribution has become smoother and the number of uncertain samples has disappeared as the training epochs increase.

**Qualitative analysis.** We conducted a qualitative analysis to examine how well RUC corrects the initial misclassification in pseudo-labels. Figure 7 compares the confusion matrices of SCAN and the SCAN+RUC for STL-10. A high concentration of items on the diagonal line confirms the advanced correction effect of RUC for every class. Figure 8 compares how the two models interpreted class traits based on the Grad-CAM [37] visualization on example images. The proposed model shows a more sophisticated prediction for similar images.

**Robustness to adversarial noise.** Clustering algorithms like SCAN introduce pseudo-labels to train the model via the Empirical Risk Minimization (ERM) method [42]. ERM is a learning principle which aims at minimizing the

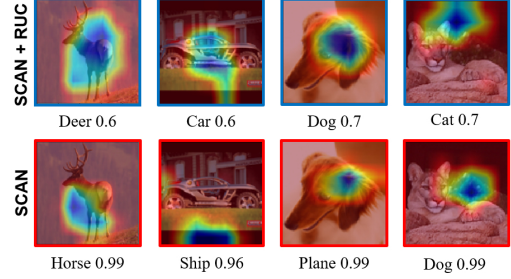


Figure 8: Class activation maps and the model’s confidence on STL-10. The high-lighted area indicates where the model focused to classify the image.

averaged error over the sampled training data (i.e., empirical risk) to find the model with small population risk (i.e., true risk). Unfortunately, ERM are known to be vulnerable to adversarial examples, which are crafted by adding visually imperceptible perturbations to the input images [30, 54].

Here, we show that RUC improves robustness against the adversarial noise. We conduct an experiment on STL-10 using adversarial perturbations of FGSM [11] and BIM [25] attacks, whose directions are aligned with the gradient of the loss surface of given samples. Figure 9 compares the model’s ability to handle the adversnoise, confirming that RUC maintain the model accuracy higher under both attack types (see the supplementary material for further details).

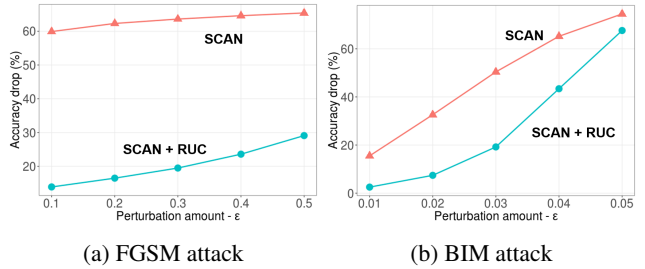


Figure 9: RUC makes the model robust to adversarial attacks, experimented with different perturbation rate  $\epsilon$ .

## 5. Conclusion

This study presented RUC, an add-on approach for improving the state-of-the-art unsupervised image clustering models via robust learning. Retraining via robust training helps avoid overconfidence and produces more calibrated clustering results. As a result, our approach demonstrated a meaningful gain on top of two state-of-the-art clustering methods. Finally, RUC helps the clustering models to be robust against adversarial attacks. We expect robust learning will be a necessary building block to advance real-world clustering solutions.



## References

- [1] Devansh Arpit, Stanislaw K Jastrzebski, Nicolas Ballas, David Krueger, Emmanuel Bengio, Maxinder S Kanwal, Tegan Maharaj, Asja Fischer, Aaron C Courville, Yoshua Bengio, et al. A closer look at memorization in deep networks. In *Proc. of International Conference on Machine Learning*, 2017. 3
- [2] Pierre Baldi. Autoencoders, unsupervised learning, and deep architectures. In *Proc. of International Conference on Machine Learning Workshop on Unsupervised and Transfer Learning*, pages 37–49, 2012. 2
- [3] Yoshua Bengio, Pascal Lamblin, Dan Popovici, and Hugo Larochelle. Greedy layer-wise training of deep networks. In *Advances in Neural Information Processing Systems*, pages 153–160, 2007. 6
- [4] David Berthelot, Nicholas Carlini, Ian Goodfellow, Nicolas Papernot, Avital Oliver, and Colin A Raffel. MixMatch: A holistic approach to semi-supervised learning. In *Advances in Neural Information Processing Systems*, pages 5049–5059, 2019. 2, 4, 5
- [5] Mathilde Caron, Piotr Bojanowski, Armand Joulin, and Matthijs Douze. Deep clustering for unsupervised learning of visual features. In *Proc. of European Conference on Computer Vision*, pages 132–149, 2018. 2, 6
- [6] Haw-Shiuan Chang, Erik Learned-Miller, and Andrew McCallum. Active bias: Training more accurate neural networks by emphasizing high variance samples. In *Advances in Neural Information Processing Systems*, pages 1002–1012, 2017. 3
- [7] Jianlong Chang, Lingfeng Wang, Gaofeng Meng, Shiming Xiang, and Chunhong Pan. Deep adaptive image clustering. In *Proc. of IEEE International Conference on Computer Vision*, pages 5879–5887, 2017. 2, 6
- [8] Ting Chen, Simon Kornblith, Mohammad Norouzi, and Geoffrey Hinton. A simple framework for contrastive learning of visual representations. In *Proc. of International Conference on Machine Learning*, 2020. 2, 4
- [9] Ekin D Cubuk, Barret Zoph, Jonathon Shlens, and Quoc V Le. Randaugment: Practical automated data augmentation with a reduced search space. In *Proc. of IEEE Conference on Computer Vision and Pattern Recognition Workshops*, pages 702–703, 2020. 5, 11
- [10] Chris Ding and Xiaofeng He. K-means clustering via principal component analysis. In *Proc. of International Conference on Machine Learning*, page 29, 2004. 1, 2
- [11] Ian J Goodfellow, Jonathon Shlens, and Christian Szegedy. Explaining and harnessing adversarial examples. In *Proc. of International Conference on Learning Representations*, 2015. 8, 12
- [12] Chuan Guo, Geoff Pleiss, Yu Sun, and Kilian Q Weinberger. On calibration of modern neural networks. In *Proc. of International Conference on Machine Learning*, pages 1321–1330, 2017. 8, 12
- [13] Divam Gupta, Ramachandran Ramjee, Nipun Kwatra, and Muthian Sivathanu. Unsupervised clustering using pseudo-semi-supervised learning. In *Proc. of International Conference on Learning Representations*, 2020. 2
- [14] Philip Haeusser, Johannes Plapp, Vladimir Golkov, Elie Aljalbout, and Daniel Cremers. Associative deep clustering: Training a classification network with no labels. In *Proc. of German Conference on Pattern Recognition*, pages 18–32. Springer, 2018. 6
- [15] Bo Han, Quanming Yao, Xingrui Yu, Gang Niu, Miao Xu, Weihua Hu, Ivor Tsang, and Masashi Sugiyama. Co-teaching: Robust training of deep neural networks with extremely noisy labels. In *Advances in Neural Information Processing Systems*, pages 8527–8537, 2018. 3, 5
- [16] Sungwon Han, Sungwon Park, Sungkyu Park, Sundong Kim, and Meeyoung Cha. Mitigating embedding and class assignment mismatch in unsupervised image classification. In *Proc. of European Conference on Computer Vision*, 2020. 1, 2, 6, 7, 11, 12
- [17] Kaiming He, Xiangyu Zhang, Shaoqing Ren, and Jian Sun. Deep residual learning for image recognition. In *Proc. of IEEE Conference on Computer Vision and Pattern Recognition*, pages 770–778, 2016. 6, 11
- [18] Dan Hendrycks, Mantas Mazeika, Duncan Wilson, and Kevin Gimpel. Using trusted data to train deep networks on labels corrupted by severe noise. In *Advances in Neural Information Processing Systems*, 2018. 3
- [19] Weihua Hu, Takeru Miyato, Seiya Tokui, Eiichi Matsumoto, and Masashi Sugiyama. Learning discrete representations via information maximizing self-augmented training. In *Proc. of International Conference on Machine Learning*, pages 1558–1567, 2017. 1, 2
- [20] Anil K Jain, M Narasimha Murty, and Patrick J Flynn. Data clustering: a review. *ACM Computing Surveys (CSUR)*, 31(3):264–323, 1999. 2
- [21] Xu Ji, Joao F Henriques, and Andrea Vedaldi. Invariant information clustering for unsupervised image classification and segmentation. In *Proc. of IEEE International Conference on Computer Vision*, pages 9865–9874, 2019. 1, 2, 6, 11
- [22] Lu Jiang, Zhengyuan Zhou, Thomas Leung, Li-Jia Li, and Li Fei-Fei. Mentornet: Learning data-driven curriculum for very deep neural networks on corrupted labels. In *Proc. of International Conference on Machine Learning*, pages 2304–2313, 2018. 3
- [23] Diederik P Kingma and Max Welling. Auto-encoding variational bayes. *arXiv preprint arXiv:1312.6114*, 2013. 2, 6
- [24] Harold W Kuhn. The hungarian method for the assignment problem. *Naval Research Logistics Quarterly*, 2(1-2):83–97, 1955. 6, 11
- [25] Alexey Kurakin, Ian Goodfellow, and Samy Bengio. Adversarial examples in the physical world. *arXiv preprint arXiv:1607.02533*, 2016. 8, 12
- [26] Junnan Li, Richard Socher, and Steven CH Hoi. Dividemix: Learning with noisy labels as semi-supervised learning. In *Proc. of International Conference on Learning Representations*, 2020. 3, 5, 7
- [27] Sheng Liu, Jonathan Niles-Weed, Narges Razavian, and Carlos Fernandez-Granda. Early-learning regularization prevents memorization of noisy labels. In *Advances in Neural Information Processing Systems*, 2020. 3

- [28] Michal Lukasik, Srinadh Bhojanapalli, Aditya Krishna Menon, and Sanjiv Kumar. Does label smoothing mitigate label noise? In *Proc. of International Conference on Machine Learning*, 2020. 2, 3, 5
- [29] Yueming Lyu and Ivor W Tsang. Curriculum loss: Robust learning and generalization against label corruption. *arXiv preprint arXiv:1905.10045*, 2019. 3
- [30] Aleksander Madry, Aleksandar Makelov, Ludwig Schmidt, Dimitris Tsipras, and Adrian Vladu. Towards deep learning models resistant to adversarial attacks. In *Proc. of International Conference on Learning Representations*, 2018. 8, 12
- [31] Eran Malach and Shai Shalev-Shwartz. Decoupling” when to update” from” how to update”. In *Advances in Neural Information Processing Systems*, pages 960–970, 2017. 3
- [32] Nagarajan Natarajan, Inderjit S Dhillon, Pradeep K Ravikumar, and Ambuj Tewari. Learning with noisy labels. In *Advances in Neural Information Processing systems*, pages 1196–1204, 2013. 3
- [33] Nicolas Papernot, Patrick McDaniel, Xi Wu, Somesh Jha, and Ananthram Swami. Distillation as a defense to adversarial perturbations against deep neural networks. In *2016 IEEE Symposium on Security and Privacy (SP)*, pages 582–597. IEEE, 2016. 13
- [34] Giorgio Patrini, Alessandro Rozza, Aditya Krishna Menon, Richard Nock, and Lizhen Qu. Making deep neural networks robust to label noise: A loss correction approach. In *Proc. of IEEE Conference on Computer Vision and Pattern Recognition*, pages 1944–1952, 2017. 3
- [35] Alec Radford, Luke Metz, and Soumith Chintala. Unsupervised representation learning with deep convolutional generative adversarial networks. In *Proc. of International Conference on Learning Representations*, 2016. 6
- [36] Matthew Schultz and Thorsten Joachims. Learning a distance metric from relative comparisons. In *Advances in Neural Information Processing Systems*, pages 41–48, 2004. 6
- [37] Ramprasaath R Selvaraju, Michael Cogswell, Abhishek Das, Ramakrishna Vedantam, Devi Parikh, and Dhruv Batra. Grad-cam: Visual explanations from deep networks via gradient-based localization. In *Proc. of IEEE International Conference on Computer Vision*, pages 618–626, 2017. 8, 13
- [38] Hwanjun Song, Minseok Kim, and Jae-Gil Lee. Selfie: Refurbishing unclear samples for robust deep learning. In *Proc. of International Conference on Machine Learning*, pages 5907–5915, 2019. 3
- [39] Hwanjun Song, Minseok Kim, Dongmin Park, and Jae-Gil Lee. Learning from noisy labels with deep neural networks: A survey. *arXiv preprint arXiv:2007.08199*, 2020. 3
- [40] Jesper E. van Engelen and Holger H. Hoos. A survey on semi-supervised learning. *Machine Learning*, 109(2):373–440, 2020. 3
- [41] Wouter Van Gansbeke, Simon Vandenhende, Stamatios Georgoulis, Marc Proesmans, and Luc Van Gool. Scan: Learning to classify images without labels. In *Proc. of European Conference on Computer Vision*, 2020. 1, 2, 6, 7, 11, 12
- [42] Vladimir Vapnik. *The nature of statistical learning theory*. Springer science & business media, 2013. 8, 12
- [43] Pascal Vincent, Hugo Larochelle, Isabelle Lajoie, Yoshua Bengio, and Pierre-Antoine Manzagol. Stacked denoising autoencoders: Learning useful representations in a deep network with a local denoising criterion. *Journal of Machine Learning Research*, 11:3371–3408, 2010. 1, 2
- [44] Jianfeng Wang, Jingdong Wang, Jingkuan Song, Xin-Shun Xu, Heng Tao Shen, and Shipeng Li. Optimized cartesian k-means. *IEEE Transactions on Knowledge and Data Engineering*, 27(1):180–192, 2014. 6
- [45] Ruxin Wang, Tongliang Liu, and Dacheng Tao. Multiclass learning with partially corrupted labels. *IEEE Transactions on Neural Networks and Learning Systems*, 29(6):2568–2580, 2017. 3
- [46] David Warde-Farley and Ian Goodfellow. 11 adversarial perturbations of deep neural networks. *Perturbations, Optimization, and Statistics*, 311, 2016. 13
- [47] Zhirong Wu, Yuanjun Xiong, Stella X Yu, and Dahua Lin. Unsupervised feature learning via non-parametric instance discrimination. In *Proc. of IEEE Conference on Computer Vision and Pattern Recognition*, pages 3733–3742, 2018. 2
- [48] Junyuan Xie, Ross Girshick, and Ali Farhadi. Unsupervised deep embedding for clustering analysis. In *Proc. of International Conference on Machine Learning*, pages 478–487, 2016. 2, 6
- [49] Yizhan Xu, Sungwon Han, Sungwon Park, Meeyoung Cha, and Cheng-Te Li. A Comprehensive and Adversarial Approach to Unsupervised Embedding Learning. In *Proc. of IEEE International Conference on Big Data*, 2020. 2
- [50] Bo Yang, Xiao Fu, Nicholas D Sidiropoulos, and Mingyi Hong. Towards k-means-friendly spaces: Simultaneous deep learning and clustering. In *Proc. of International Conference on Machine Learning*, pages 3861–3870, 2017. 2
- [51] Jianwei Yang, Devi Parikh, and Dhruv Batra. Joint unsupervised learning of deep representations and image clusters. In *Proc. of IEEE Conference on Computer Vision and Pattern Recognition*, pages 5147–5156, 2016. 6
- [52] Xingrui Yu, Bo Han, Jiangchao Yao, Gang Niu, Ivor Tsang, and Masashi Sugiyama. How does disagreement help generalization against label corruption? In *Proc. of International Conference on Machine Learning*, pages 7164–7173, 2019. 3
- [53] Lihi Zelnik-Manor and Pietro Perona. Self-tuning spectral clustering. In *Advances in Neural Information Processing Systems*, pages 1601–1608, 2005. 6
- [54] Hongyi Zhang, Moustapha Cisse, Yann N Dauphin, and David Lopez-Paz. mixup: Beyond empirical risk minimization. In *Proc. of International Conference on Learning Representations*, 2018. 4, 5, 8, 12

## A. Supplementary Material

### A.1. Release

Codes, training details, and the downloadable link for trained models are available via an anonymized github repository: <https://github.com/deu30303/RUC>.

### A.2. Training Details

Our model employed the ResNet18 [17] architecture following other baselines [16, 21, 41]. Before retraining, note that we randomly initialize the final fully connected layer or replace the backbone network with a newly pretrained one from an unsupervised embedding learning algorithm like SimCLR. This random re-initialization process helps avoid the model falling into the same local optimum as the original model does. Initial confidence threshold  $\tau_1$  was set as 0.99, and the number of neighbors  $k$  to divide the clean and noise samples was set to 100. The threshold  $\tau_2$  for refurbishing started from 0.9 and increased by 0.02 in every 40 epochs. The label smoothing parameter  $\epsilon$  was set to 0.5. The initial learning rate was set as 0.01, which decays smoothly by cosine annealing. The model was trained for 200 epochs using SGD with a momentum of 0.9, a weight decay of 0.0005. Batch size was 100 for STL-10 and 200 for CIFAR-10 and CIFAR-20. We chose  $\lambda_u$  as 25, 50, 100 for CIFAR-10, STL-10 and CIFAR-20.  $w_b$  was calculated by applying min-max normalization to confidence value of the counter network  $f_{\theta(c)}$ . Random crop and horizontal flip were used as a weak augmentation, which does not deform the image’s original form. RandAugment [9] was used as a strong augmentation. We report all transformation operations for strong augmentation strategies in Table 4. Number of transformations and magnitude for all the transformations in RandAugment was set to 2.

Transformation	Parameter	Range
AutoContrast	-	-
Equalize	-	-
Identity	-	-
Brightness	$B$	[0.01, 0.99]
Color	$C$	[0.01, 0.99]
Contrast	$C$	[0.01, 0.99]
Posterize	$B$	[1, 8]
Rotate	$\theta$	[-45, 45]
Sharpness	$S$	[0.01, 0.99]
Shear X, Y	$R$	[-0.3, 0.3]
Solarize	$T$	[0, 256]
Translate X, Y	$\lambda$	[-0.3, 0.3]

Table 4: List of transformations used in RandAugment.

For evaluating the class assignment, Hungarian method [24] was used to map the best bijection permutation between the predictions and ground-truth. We also note that computational cost of RUC is not a big burden. It took

less than 12 hours to run 200 epochs with 4 TITAN Xp for all datasets.

### A.3. Hyper-parameters of Sampling Strategies

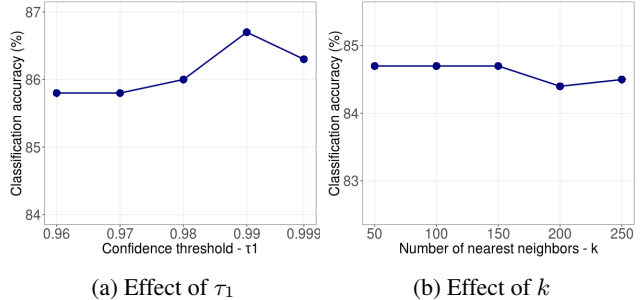


Figure 10: Analysis of the accuracy on the STL-10 dataset across two hyper-parameters: (a)  $\tau_1$  from the confidence-based strategy and (b)  $k$  from the metric-based strategy.

Hyper-parameters can affect the final classification accuracy of our clustering model. We investigate the effect of hyper-parameters from two sampling strategies:  $\tau_1$  and  $k$ .  $\tau_1$  is a threshold for selecting clean samples in the confidence-based strategy, while  $k$  is the number of neighbors for kNN classifier in the metric-based strategy. Figure 10 summarizes the effect of each hyper-parameter respectively. In the case of  $\tau_1$ , the final accuracy reaches the highest at  $\tau_1 = 0.99$  and starts to decrease. Small  $\tau_1$  extracts clean samples with higher recall and lower precision, while large  $\tau_1$  extracts clean samples with higher precision and lower recall. Hence, balancing between the precision and recall through appropriate  $\tau_1$  can lead to better performance. Meanwhile, the number of nearest neighbors  $k$  does not significantly affect the final accuracy. Given  $k$  within the reasonable range, our model consistently produces results with high performance.

### A.4. Additional Analysis for RUC on TSUC

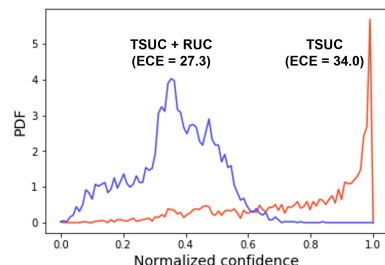


Figure 11: Confidence distribution for noise sample on STL-10 with the base model TSUC.

Many recent unsupervised clustering algorithms are subject to overconfident results because of their entropy-based

balancing [16, 41]. If a model is overconfident to noisy samples, separating the clean set and the unclean set becomes challenging, and this can induce the overall performance degradation. We conduct an experiment to evaluate the calibration effect of RUC on top of TSUC (See Figure 11). TSUC’s confidence is highly concentrated near 1, while our model’s confidence is widely distributed. We also report the degree of calibration quality using Expected Calibration Error (ECE) [12]:

$$\text{ECE} = \sum_{m=1}^M \frac{|B_m|}{n} |acc(B_m) - conf(B_m)|, \quad (21)$$

where  $n$  is the number of data points,  $B_m$  is the  $m$ -th group from equally spaced buckets based on the model confidence over the data points;  $acc(B_m)$  and  $conf(B_m)$  are average accuracy and confidence over  $B_m$  respectively. TSUC’s high ECE implies that TSUC is much more overconfident than SCAN. Lower ECE of TSUC + RUC in Figure 11 implies that our add-on process leads to better calibrations.

We also evaluate the quality of the clean set from TSUC generated from three sampling strategies. The results are shown in Table 5. Overall, the precision is higher for the hybrid strategy, whereas the recall is higher for the metric-based strategy as same as the SCAN’s results. Meanwhile, confidence-based strategies in TSUC showed low precision, which implies that TSUC is not well calibrated and highly overconfident.

Strategy	CIFAR-10			CIFAR-20			STL-10		
	C	M	H	C	M	H	C	M	H
Precision	80.9	84.2	82.7	40.9	41.8	43.0	68.2	69.0	71.4
Recall	69.9	96.4	68.0	47.4	90.3	45.5	78.3	79.4	76.2
F1 Score	69.5	89.9	74.6	43.9	85.5	44.2	72.9	73.8	73.7

Table 5: Quality of the clean set (C : Confidence, M : Metric, H : Hybrid)

### A.5. Further Discussion on Co-Training

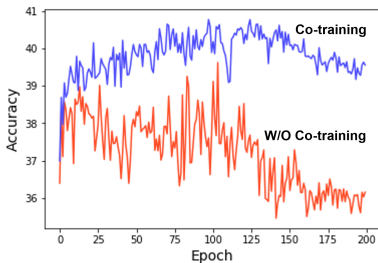


Figure 12: Changes of clustering accuracy across each epoch on CIFAR-20 with the base model TSUC.

Our model architecture introduces a co-training module

where the two networks exchange their guesses for teaching each other via co-refinement. Due to the different learning abilities in two networks, disagreements from networks help filter out corrupted labels, and we found this contributes to a substantial performance increase in unsupervised classification. Besides, the co-training structure provides extra stability in the training process.

Figure 12 compares our model and the same model without co-training based on classification accuracy across the training epoch. The model without co-training shows large fluctuations in accuracy; in contrast, the full model’s accuracy remains stable and consistent throughout epochs. We speculate this extra stability comes from our model’s ensemble architecture and the effect of loss correction. Corrected labels via ensemble predictions bring additional label smoothing, and thereby, it may reduce the negative training signals from unclean samples, which can lead to abrupt updates on the model parameters.

### A.6. Further Details on Adversarial Robustness

Empirical risk minimization (ERM), a learning principle which aims to minimize the averaged error over the sampled training data (i.e., empirical risk), has shown remarkable success as a recipe to find the model with small population risk (i.e., true risk) in supervised setting [42]. However, ERM-based training is also known to lead the model to memorize the entire training data, and often does not guarantee to be robust on adversarial noise [30, 54]. This weakness can also be inherited from several unsupervised clustering algorithms that introduce the ERM principle with their pseudo-labels, like SCAN [41].

Adding RUC to the existing clustering models improves robustness against adversarial noise. To demonstrate this, we conducted an experiment using adversarial perturbations of the FGSM [11] and BIM [25] attacks, whose directions are aligned with the gradient of the loss surface of given samples. The details of each attack are as follows:

**Fast Gradient Sign Method (FGSM)** FGSM crafts adversarial perturbations by calculating the gradients of the loss function  $J(\theta, \mathbf{x}, \mathbf{y})$  with respect to the input variables. The input image is perturbed by magnitude  $\epsilon$  with the direction aligned with the computed gradients (Eq. (22)).

$$\mathbf{x}^{adv} = \mathbf{x} + \epsilon \cdot \text{sgn}(\nabla_{\mathbf{x}} J(\theta, \mathbf{x}, \mathbf{y})) \quad (22)$$

**Basic Iterative Method (BIM)** BIM is an iterative version of FGSM attack, which generates FGSM based adversarial noise with small  $\epsilon$  and applies the noise many times in a recursive way (Eq. (24)).

$$\mathbf{x}_0^{adv} = \mathbf{x} \quad (23)$$

$$\mathbf{x}_i^{adv} = \text{clip}_{\mathbf{x}, \epsilon}(\mathbf{x}_{i-1}^{adv} + \epsilon \cdot \text{sgn}(\nabla_{\mathbf{x}_{i-1}^{adv}} J(\theta, \mathbf{x}_{i-1}^{adv}, \mathbf{y}))) \quad (24)$$



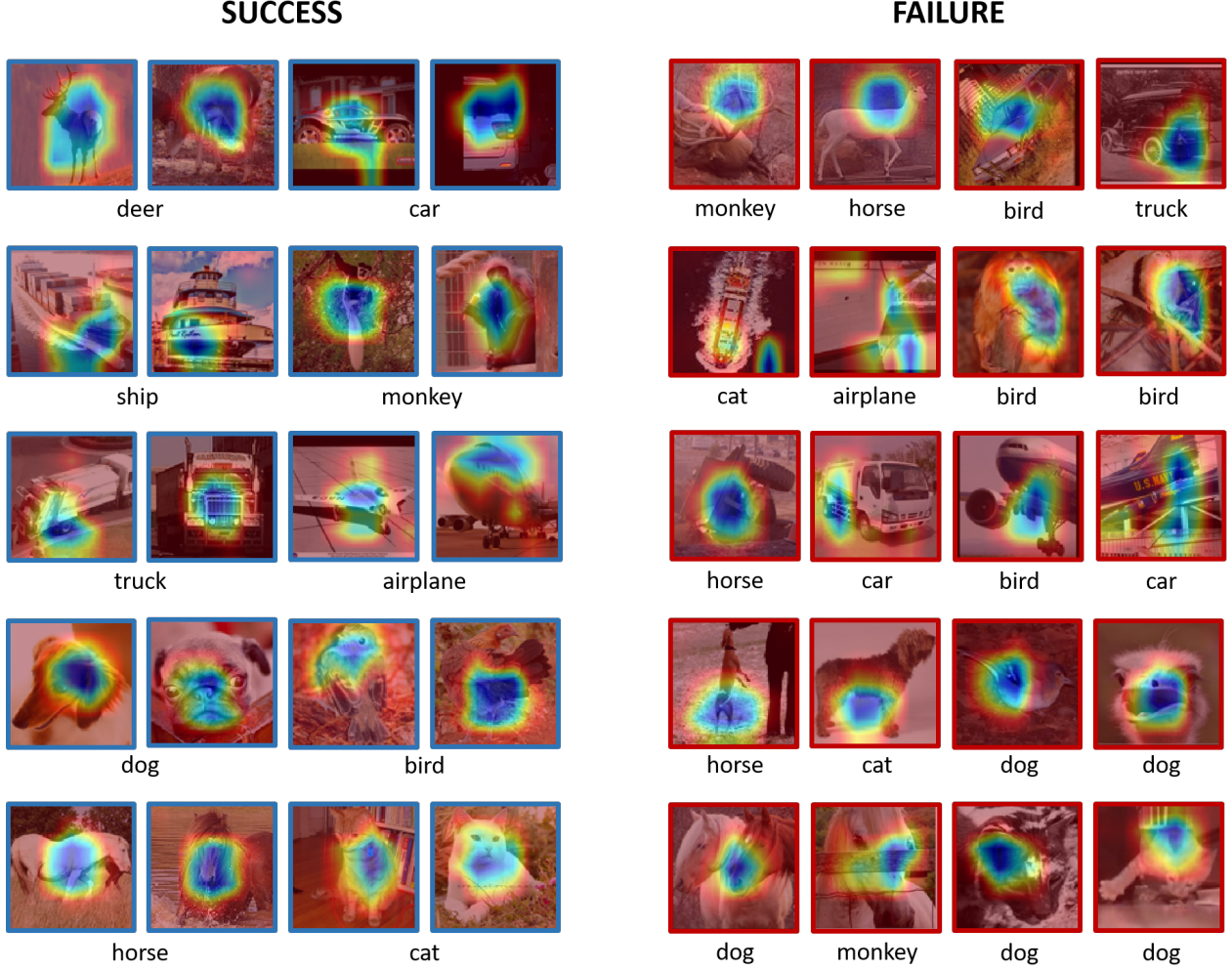


Figure 13: Additional example of successes and failures from STL-10 where the highlighted part indicates how the model interprets class traits based on the Grad-CAM. (Blue frame: success case, Red frame: failure case)

Clip function maintains the magnitude of noise below  $\epsilon$  by clipping. For BIM attack experiments, we use five iterations with an equal step size.

Figure 9 in our main manuscript compares the model’s ability to handle adversarial attacks, which confirms that adding RUC helps maintain the model accuracy better for both attack types. An investigation could guide us that this improved robustness is mainly due to the label smoothing techniques, which regularize the model to avoid overconfident results and reduce the amplitude of adversarial gradients with smoothed labels [33, 46].

### A.7. Additional Examples for Qualitative Analysis

Figure 13 shows additional examples for the visual interpretation from RUC on top of SCAN via Grad-CAM algorithm [37]. Blue framed images are the randomly chosen success cases from STL-10. In contrast, red framed images are the randomly chosen failure cases. Overall, the network trained with our model can extract key features from the images. Even though the model sometimes fails, most of the failures occurred between similar classes (e.g., horse-deer, cat-dog, truck-car, dog-deer)